Chemosphere 238 (2020) 124630

Contents lists available at ScienceDirect

Chemosphere

journal homepage: www.elsevier.com/locate/chemosphere

Newly deposited atmospheric mercury in a simulated rice ecosystem in an active mercury mining region: High loading, accumulation, and availability

Ming Ao [a, b, c], Xiaohang Xu [b, d], Yonggui Wu [c, **], Chao Zhang [b], Bo Meng [b], Lihai Shang [b], Longchao Liang [b, c], Rongliang Qiu [a], Shizhong Wang [a], Xiaoli Qian [c], Lei Zhao [b], Guangle Qiu [b, *]

[a] School of Environmental Science and Engineering, Sun Yat-sen University, Guangzhou, 510275, PR China
[b] State Key Laboratory of Environmental Geochemistry, Institute of Geochemistry, Chinese Academic of Sciences, Guiyang, 550081, PR China
[c] College of Resources and Environmental Engineering, Guizhou University, Guiyang, 550025, PR China
[d] University of Chinese Academy of Sciences, Beijing, 100049, PR China

HIGHLIGHTS

- Cinnabar retorting causes significant Hg emissions into the surrounding environment.
- Approximately 85% of the TGM emitted from the Hg smelter is deposited within a distance of 6.0 −12 km.
- The newly deposited TGM is bioavailable, readily methylated, and easily taken up by rice.

GRAPHICAL ABSTRACT

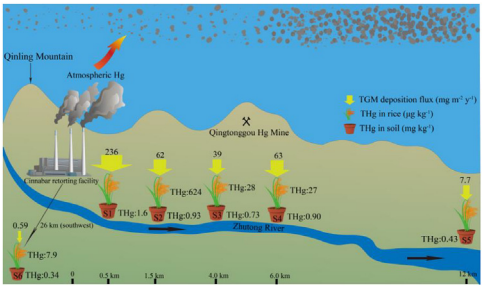

ARTICLE INFO

Article history:
Received 23 June 2019
Received in revised form
17 August 2019
Accepted 20 August 2019
Available online 24 August 2019

Handling Editor: Lena Q. Ma

Keywords:
Newly deposited atmospheric mercury
Simulated rice ecosystem
Active mercury mining activity

ABSTRACT:

Mercury (Hg) mining activities are an important anthropogenic source of atmospheric Hg. The Xunyang Hg mine located in Shaanxi Province is the largest active Hg producing centre in China. To understand the biogeochemical processes of atmospheric Hg through Hg mining activities, six groups of experimental pots were carefully designed to investigate the effect of Hg mining activities on Hg contamination from atmospheric deposition in the local surface soils. Based on the variations of Hg in the soil from the experimental pots, the deposition flux and loading of Hg in the Xunyang Hg mining district were investigated. The results showed that the average concentration of total gaseous mercury (TGM) as high as 193 ± 122 ng m^{-3} was observed in the ambient air, which was orders of magnitude higher than that in remote areas. The average deposition flux and annual loading of atmospheric Hg were 72 mg m^{-2} y^{-1} and 10 t y^{-1}, respectively. The dominant atmospheric Hg deposition is within a distance range of 6.0 −12 km from the Hg retorting facility, accounting for approximately 85% of the total Hg loading. After 14 months of exposure, total mercury (THg) concentrations in the soil from the experimental pots increased 0.35–9.5 times, and the highest concentrations of methylmercury (MeHg) (3.7 ± 2.9 μg kg^{-1}) in soil were observed in February. Concentrations as high as 643 μg kg^{-1} THg and 13 μg kg^{-1} MeHg in rice were observed in the second experimental year. Elevated concentrations of both THg and MeHg in rice indicated that the newly deposited atmospheric Hg was bioavailable, readily methylated, and taken up

* Corresponding author.
** Corresponding author.
E-mail addresses: ygwu72@126.com (Y. Wu), qiuguangle@vip.skleg.cn (G. Qiu).

https://doi.org/10.1016/j.chemosphere.2019.124630

by rice, suggesting that the ongoing Hg mining activities cause serious Hg contamination in the soil-rice ecosystem and posed a threat to local residents in the Xunyang Hg mining area.

1. Introduction

Mercury (Hg) is a global pollutant and an acute neurotoxin (Lindqvist et al., 1991). As a unique heavy element that can exist in an elemental form (Hg^0), Hg exists largely as Hg^0 plus trace amounts of divalent gaseous Hg and particulate Hg in the atmosphere (Galbreath and Zygarlicke, 1996). The atmospheric residence time of Hg^0 is several months to more than one year (Schroeder and Munthe, 1998; Weiss-Penzias et al., 2003; Sprovieri et al., 2010). Both divalent gaseous Hg and particulate Hg (<5% of total atmospheric Hg) have much shorter residence time (a few days to weeks) and tend to be deposited locally through wet and dry deposition (Wang et al., 2018). Natural processes and anthropogenic activities can release Hg into the atmosphere. Previous studies have demonstrated that modern global Hg contamination is dominated by anthropogenic activities, such as fossil-fuel fired power plants, non-ferrous metal smelting and cement production, etc. (Liu et al., 2019).

Industrial activities have increased global Hg emissions approximately 3-fold since preindustrial times (Jaffe and Strode, 2008). Current global atmospheric anthropogenic emissions of Hg into the atmosphere was estimated to be $2500 \pm 500\ t\ y^{-1}$ (Outridge et al., 2018). The total anthropogenic Hg emissions were estimated to be continuously increasing from 356 t in 2000 to 538 t in 2010, with an average annual increasing rate of 4.2% in China (Zhang et al., 2015). Hg mining and smelting activities are considered to be significant sources of Hg released to the atmosphere (Qiu et al., 2012, 2013; Zhang et al., 2015; Outridge et al., 2018). High-elevation atmospheric Hg quickly comes back to the earth's surface through wet and dry deposition (Schroeder and Munthe, 1998; Driscoll et al., 2013). Once deposited, Hg can be transformed under anoxic conditions into methylmercury (MeHg) (Lindberg et al., 2007), the most toxic form of Hg that can severely afflict the nervous system and unborn foetuses (Clarkson et al., 2003). Previous studies have indicated that newly deposited Hg is more reactive than native Hg with respect to methylation and that newly formed MeHg is easily absorbed by organisms and enters the food chain (Hintelmann et al., 2002; Mahaffey et al., 2004; Branfireun et al., 2005; Gibb et al., 2011).

Rice growing in heavily Hg-contaminated sites has been demonstrated to bioaccumulate as high as 174 $\mu g\ kg^{-1}$ MeHg in rice grains and becomes another major pathway of MeHg exposure to residents (Qiu et al., 2008; Feng et al., 2008; Zhang et al., 2010a; Li et al., 2012a). Unlike root transfer of the original Hg in soils, which has been extensively studied (Beckers and Rinklebe, 2017), there is a lack of knowledge regarding the biogeochemistry of newly deposited Hg inputted to rice-paddy soil systems from atmospheric deposition (Meng et al., 2012).

The Xunyang Hg mine in Shaanxi Province is currently the largest active Hg producing centre in China. The total reserves of cinnabar ore in the Xunyang Hg mine have reached 14,000 t of Hg. Historical Hg mining activities in the Xunyang area can be dated back to 770–221 BC. Presently, there are two cinnabar ore mines and one retorting factory in the Xunyang mining area. Studies have reported that the anomalously high total Hg (THg) concentrations in soils have reached 750 $mg\ kg^{-1}$ (Zhang et al., 2009) and that the MeHg concentrations in paddy soils and rice near Hg mining sites have reached as high as 11 $\mu g\ kg^{-1}$ and 80 $\mu g\ kg^{-1}$, respectively (Qiu et al., 2011, 2012). Abnormally high elevated concentrations of total gaseous mercury (TGM) in the Xunyang Hg mining district were also observed, ranging from 24 to 2220 $ng\ m^{-3}$, with an average of 302 $ng\ m^{-3}$ (Ao et al., 2017). Elevated levels of TGM may result in high Hg deposition rates for the surroundings, providing a favourable opportunity to obtain better understanding of the biogeochemistry of newly deposited Hg in rice ecosystems.

Here, we select the active Hg mining district in Xunyang, China to better understand the effects of newly deposited Hg on rice ecosystems. The concentrations of THg and MeHg in soils and rice from in situ simulated rice ecosystems, as well as TGM concentrations in the ambient air, were measured during the experimental period. The objectives were to (1) estimate the Hg deposition fluxes and loading in the study region and (2) characterize THg and MeHg distribution and bioaccumulation in a simulated rice ecosystem influenced by the newly deposited atmospheric Hg.

2. Study area

Xunyang County (N: 32°51′38″~33°05′23″, E: 109°23′31″~109°31′31″) is located in southeast Shaanxi Province, central China and covers approximately 1000 km^2 (Fig. 1). It has a typical mountainous topography with elevations ranging from 185 to 2358 m. The study area has a northern, subtropical humid climate characterized with abundant rainfall and mild temperatures. The annual average rainfall is approximately 851 mm, and the annual mean temperature is 15.4 °C. The rainy season primarily occurs from May to September. The prevailing wind directions are primarily to the south and to the east in the study area. The Zhutong and Shengjia Rivers are two major tributaries of the Shu River that flow through the Hg mining area. The Shu River flows into the Han River, which is a large tributary of the Yangtze River.

The Xunyang Hg mining district consists of the Qingtonggou (QTG) mine and Gongguan (GG) mine, and the Hg deposits are hosted by dolomite strata in the Devonian (Zhang et al., 2010b). The Hg deposits were formed in the stage of volcanism. The Hg ore body is controlled jointly by the fold structure (anticline) and fracture structure (Zhang et al., 2010b). The ore body is veined, and the ore is composed of cinnabar, stibnite, quartz and calcite. An approximate total metal Hg production from the Xunyang Hg mine was estimated to be 3000 $t\ y^{-1}$ in the 1990s and has presently decreased to approximately 350 $t\ y^{-1}$. The QTG mine is located in the midstream of the Zhutong River, and the GG mine is located on the west side of the watershed. The Hg retorting facility is located upstream of the Zhutong River. The smelting recovery was approximately 95%, and the remaining 5% of total Hg was lost into the atmosphere or was dumped as a byproduct into the river.

3. Methods and materials

3.1. Experimental design

3.1.1. Site selection

Six sites noted as S1, S2, S3, S4, S5 and S6 were selected to evaluate the effects of TGM deposition from Hg mining and retorting on simulated rice ecosystems. S1 to S5 were distributed

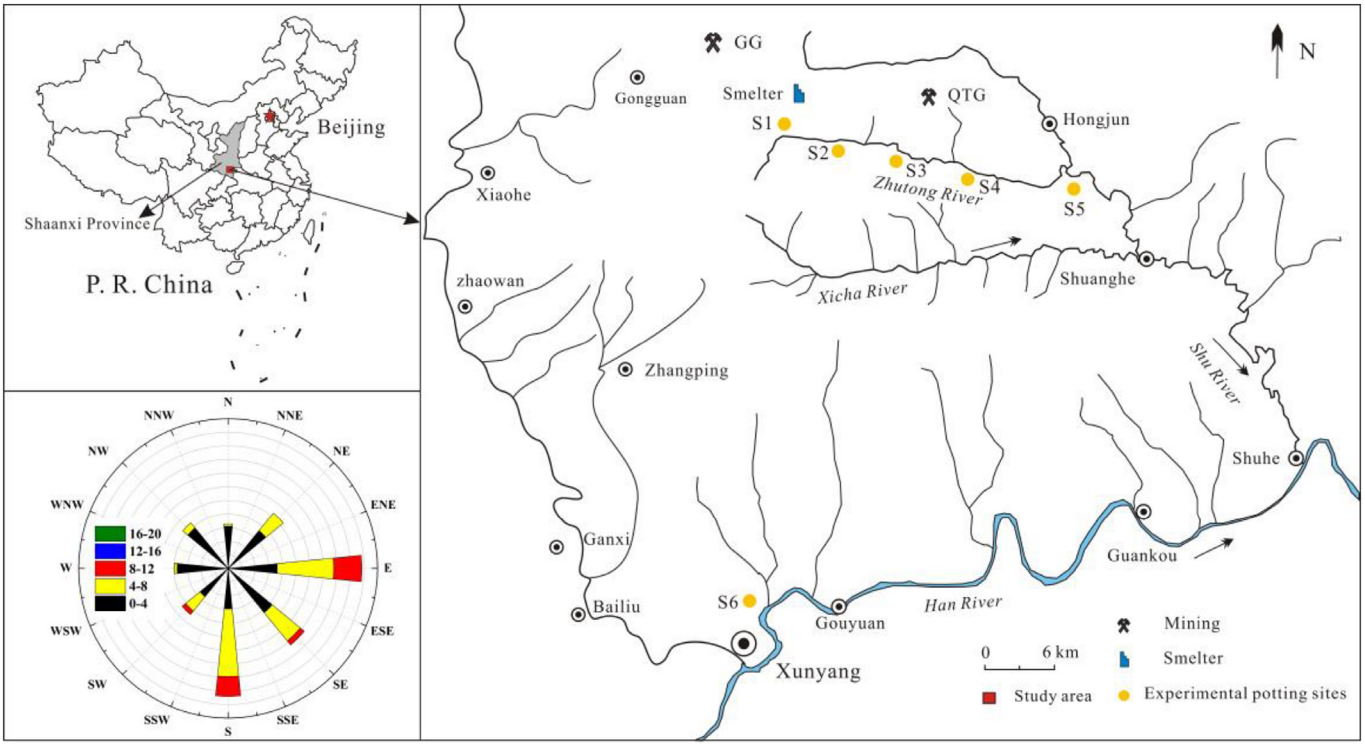

Fig. 1. The study area and locations of experimental potting sites (Rose diagram indicates wind directions during the sampling periods in the study region).

along the Zhutong River and characterized with gradient atmospheric Hg (Qiu et al., 2012), and S6, approximately 26 km south of the Hg retorting facility, was selected as the control site. The Hg retorting facility lies in the north of site S1, and the QTG Hg mining pit lies to the north between S3 and S4. In detail, S1 was located approximately 0.5 km downwind from the Hg retorting facility, approximately 1.5 km for S2, 4.0 km for S3, 6.0 km for S4, and 12 km for S5. S6 was adjacent to the suburban town of Xunyang.

3.1.2. Experimental pots

Self-designed experimental receiver pots (a wooden box with dimensions of length × width × height = 30 × 30 × 40 cm) for atmospheric deposition were used in the simulated rice ecosystems. The volume of each of the experimental pots was 0.036 m^3, with an open receiving area of 0.09 m^2. The boxes were constructed of wood to avoid light, and the insides were constructed with impermeable plastic to prevent leaching (Fig. S1). At each experimental site, triple-duplicate pots were set, each of which was filled with natural paddy soil having low Hg levels. The soil (original soil) was collected from a control site in Huaxi, Guizhou Province, China, that had low level of THg (0.34 ± 0.011 mg kg^{-1}). The average MeHg concentration in this soil was 0.38 ± 0.09 μg kg^{-1}. The mean concentration of organic matter in the soil was 5.8 ± 0.26%, and the mean pH value was 6.1 ± 0.32. The depth of the soil in each pot was approximately 20 cm.

Prior to experimental pot filling, the soil was air-dried, ground to 10 meshes per inch, and thoroughly mixed. Each experimental pot was filled with 15 kg soil and then irrigated with local drinking water containing a low concentration of Hg (4.7 ± 1.4 ng L^{-1}). All experimental pots were placed in an open space that was not disturbed by human activities and litterfall at each site. A rice cultivar (*Oryza sativa* L.) widely grown in Shaanxi Province was selected for the investigation. Three individual rice seedlings were transplanted in each pot annually during the rice growing season. To maintain flooded soil conditions, approximately 2–4 cm of water above the soil surface was required during the whole rice-growing period. The field experiments started in June 2012 and ended in August 2013. Two harvest seasons of rice were achieved for 2012 and 2013.

3.2. Sampling and preparation

Soil samples were collected every two months from June 2012 to August 2013, and a total of 144 samples were collected from the six sites of experimental pots. During sampling, only 0–10 cm topsoil was collected to avoid influencing the rice growth. Each soil sample was collected by hand with a disposable polyethylene glove. The final soil sample (250 g) was composed of 5 sub-samples within an experimental pot following the diagonal sampling technique. The soils were sealed and double-bagged in situ to avoid cross-contamination and then transported in an ice-cooled container to a refrigerator (−18 °C) within 24 h. In the laboratory, the soils were freeze-dried, homogenized, and ground to a size of 200 meshes per inch for analysis.

A total of 30 rice samples (grains) were collected from the six sites of experimental pots during two rice harvest seasons in 2012 and 2013. All rice samples were sealed and stored in hop-pockets to avoid cross-contamination. In the laboratory, the grains were freeze-dried. Then the hulls of the grains were removed. After that, the brown rice was polished to remove bran to produce white rice with a rice mill. Finally, the white rice was ground to a powder with a grinder (IKA-A11, Germany) and stored in plastic bags for analysis.

Corresponding TGM concentrations in the ambient air were measured using the Lumex RA-915 + Portable Mercury Vapor Analyzer (Lumex Ltd, Russia) corresponding to each soil sampling campaign. This instrument is based on the Zeeman cold vapor atomic absorption spectrometry technique with a detection limit for Hg in the ambient air of 0.5 ng m^{-3} at a rate of 10 L min^{-1}.

Average TGM concentrations during a 20 s interval were retrieved and stored in a portable computer. Measurements at each sampling site were continuously carried out for at least 30–60 min.

3.3. Measurements

3.3.1. Soil

For soil THg analysis, approximately 0.1–0.2 g of dry sample was digested at 95 °C with freshly prepared aqua regia HCl/HNO_3 (v/v, 3:1) for 30 min; then, 0.5 ml BrCl was added, and the mixture was heated to 95 °C for 3 h. Afterwards, an aliquot of digested sample solution and 0.4 mL 20% $SnCl_2 \cdot 2H_2O$ were added into the bubbler and then measured by a F732–V; the detection limit for THg in the sample was 0.05 μg L^{-1}.

For soil MeHg determination, approximately 0.2–0.3 g of a dry soil sample was leached with 2 mol L^{-1} $CuSO_4 \cdot 5H_2O$ and 25% HNO_3. Then, MeHg in the sample was extracted with dichloromethane (CH_2Cl_2) as well as back-extracted from the solvent phase into water and aqueous phase ethylation. MeHg was separated from the digested solution by purging with N_2 onto a Tenax trap. Afterwards, a suitable aliquot of digested sample solution was measured by gas chromatography cold vapor atomic fluorescence spectrometry (GC-CVAFS) (Liang et al., 2004).

3.3.2. Rice

For the rice THg measurement, approximately 0.2–0.3 g of dry sample was digested using HNO_3/H_2SO_4 (v/v, 4:1) in a water bath (95 °C) for 3 h; then, BrCl was added into the digested solution before determination. An appropriate aliquot was added into the bubbler for $SnCl_2$ reduction, purging and gold-trap collection (Xu et al., 2017). Afterwards, the Hg on the gold trap was measured using cold vapor atomic fluorescence spectroscopy (CVAFS).

For rice MeHg analysis, approximately 0.2–0.5 g of a dry rice sample was digested using 25% KOH-methanol in a water bath (75 °C) for 3 h. The digestive solution was then acidified with concentrated HCl. After that, MeHg in the sample was extracted with CH_2Cl_2 as well as back-extracted from the solvent phase into water and aqueous phase ethylation. Afterwards, MeHg was separated from the digested solution by purging with N_2 onto a Tenax trap. A suitable aliquot of digested sample solution was measured by GC-CVAFS (Liang et al., 1996).

Previous studies have reported that, except for MeHg, other organic Hg forms, such as ethyl Hg, could not be detected in rice, wheat, and dogfish samples (Lin et al., 2008), suggesting their much lower concentrations. The sum of the concentrations of inorganic mercury (IHg) and MeHg agreed with the THg concentrations of Hg determined in those types of samples (Lin et al., 2008). Hence, in the present study, the concentrations of IHg in rice were defined as the differences between the concentrations of THg and MeHg in rice, which will be discussed in Section 4.3.

3.4. QA/QC

Quality assurance and quality control of THg and MeHg determination in samples was performed using duplicates, method blanks, a matrix and certified reference materials (PACS-2; ERM-CC580; GBW10020; TORT-2). The method detection limits were 10 ng kg^{-1} for THg and 2 ng kg^{-1} for MeHg in the soil and rice samples.

The analytical accuracy for THg in soil was estimated from an analysis of the sediment quality standard of PACS-2, with values obtained of 3.01 ± 0.05 mg kg^{-1} (n = 5) compared with the certified value of 3.02 ± 0.20 mg kg^{-1}. The analytical accuracy for MeHg in soil was estimated from analyses of the sediment quality standard of ERM-CC580, and the achieved MeHg concentration of 75.2 ± 2.9 μg kg^{-1} (n = 5) was compared with the certified value of 75.5 ± 4.0 μg kg^{-1}. The recoveries of certificated reference materials were in the range of 96.5%~101.3% and 91.4%~108.3% for THg and MeHg, respectively. In soil duplicates, the relative percent difference was less 9.4% for THg and 8.3% for MeHg.

The analytical accuracy for THg in rice was estimated from an analysis of the plant standard substance GBW10020, with obtained values of 148 ± 3.0 μg kg^{-1} (n = 5), which are comparable with the certified value of 150 ± 20 μg kg^{-1}. MeHg concentrations measured in rice were estimated from analyses of the biological standards of TORT-2, with obtained values of 136 ± 4.0 μg kg^{-1} (n = 5), whose reference value is 137 ± 12 μg kg^{-1}. The recoveries of certificated reference materials were in the range of 95.9% ~97.9% and 91.2%~105.3% for THg and MeHg, respectively. In rice duplicates, the relative percent difference was less 7.5% for THg and 8.6% for MeHg.

3.5. Estimation of TGM deposition flux

Based on the temporal concentrations of Hg in soils collected from the experimental pots, monthly atmospheric Hg deposition fluxes and annual Hg loading during the sampling periods were estimated by referring to Ferrat et al. (2012). The estimation method was as follows in Eq (1). The annual total Hg loading from the retorting facility was estimated as follows in Eq (2).

$$F_{Hg} = (C_n - C_{n-1}) \times m \div S \div \Delta t \times 365 \quad (1)$$

$$M = F_{Hg} \times \Delta S_n \div 10^9 \quad (2)$$

where.

F_{Hg} is the TGM deposition flux at different sampling times (mg m^{-2} y^{-1});
n is the sampling time (n = 1, 2, 3, 4, 5, 6, 7);
C_0 is the Hg concentration in the original experimental soils (0.34 ± 0.011 mg kg^{-1});
C_n is the Hg concentration in the experimental soil at the end of the elapsed time (mg kg^{-1});
C_{n-1} is the Hg concentration in the experimental soil at the beginning of the elapsed time (mg kg^{-1});
m is the weight of the soil (0–10 cm depth, 7.5 kg);
S is the area receiving TGM deposition (0.09 m^2);
$\triangle t$ is the time elapsed (day); and 365 is the unit conversion factor for one year;
M is the deposition Hg loading (t y^{-1});
$\triangle S_n$ is the deposition area between the two adjacent experimental sites (m^2); and
10^9 is a unit conversion factor.

It should be noted that the Xunyang Hg mining district was divided into six specific subareas based on the location of the Hg retorting facility (TGM emitter source) and the six selected experimental sites. The location of the Hg retorting facility was treated as the TGM emission centre, and the distances between the Hg retorting facility and the experimental site was treated as the circle radius. The specific area was calculated by the difference in area between two adjacent experimental sites. For example, when n = 1, $\triangle S_n$ is the circular area with a radius with the Hg retorting facility to S1; when n = 2, $\triangle S_n$ is the area difference between the area within S2 and S1.

4. Results and discussion

4.1. Air

4.1.1. TGM in ambient air

The average (range) TGM concentrations at sites S1, S2, S3, S4 and S5 were 77 ± 82 (2.6–370) ng m^{-3}, 193 ± 122 (62–537) ng m^{-3}, 32 ± 27 (1.7–108) ng m^{-3}, 41 ± 37 (8.4–173) ng m^{-3} and 16 ± 17 (2.0–61) ng m^{-3}, respectively (Table 1). High values of TGM were found near the Hg retorting facility, confirming that the Hg retorting facility was the dominant TGM emitter in the region. As expected, the lowest TGM concentrations were observed at control site S6 and ranged from 2.1 to 15 ng m^{-3}, with an average of 5.7 ± 2.7 ng m^{-3}. Our results showed that the TGM concentrations in the Xunyang Hg mining district (S1–S5) were 2.8–34 times higher than those observed in a remote area (S6). The TGM concentrations in the ambient air at site S6 were similar to the range of 5–13 ng m^{-3} in the outskirts and residential areas (Li et al., 2014; Ma et al., 2015), reflecting the lower impact by the retorting activities but showing a possible contribution from local fossil fuel combustion (Wu et al., 2006; Wan et al., 2009a; Liu et al., 2011). Because site S6 was located in a remote village, and coal is major energy source in rural area in Shaanxi, approximately 25% of total coal consumption originated from domestic coal burning for cooking and household heating (ShaanxiStatistical Yearbook, 2012). In addition, the mean Hg concentration in coal from Shaanxi Province (0.25 mg kg^{-1}) is slightly higher than the national average value in China (0.17 mg kg^{-1}) (Zhang et al., 2012). The second source may be from the human activities in the surrounding area at S6, such as building and traffic dust (Wang et al., 2018).

The average TGM concentration of 193 ng m^{-3} at experimental site S2 decreased rapidly to 16 ng m^{-3} at experimental site S5 within a distance of 1.5 km–12 km from the Hg retorting facility. Meanwhile, large variations in the temporal distribution patterns among seasons were detected. The TGM concentrations in spring, summer and autumn (64 ng m^{-3}, 73 ng m^{-3} and 80 ng m^{-3}, respectively) were significantly higher than those in winter (26 ng m^{-3}). Compared to the TGM concentrations in other Hg mining districts worldwide, such as Wanshan (12–1652 ng m^{-3}, Wang et al., 2007), Wuchuan (10–40000 ng m^{-3}, Li et al., 2012b) and Idrija (~5000 ng m^{-3}, Kocman et al., 2011), the TGM concentrations in the ambient air in the Xunyang Hg mining district were slightly lower but were at similar orders of magnitude. However, the TGM concentrations in the ambient air in the Xunyang Hg mining district were significantly higher than the values observed in the remote mountainous areas unaffected by Hg pollution, such as Waliguan Mountain (1.98 ± 0.98 ng m^{-3}, Fu et al., 2012), Jinyun Mountain (4.2 ± 2.6 ng m^{-3}, Ma et al., 2015) and urban areas (6.2 ± 5.1 ng m^{-3}, Liu et al., 2011). The elevated TGM levels in the ambient air undoubtedly imply high TGM deposition for the surrounding environment.

4.1.2. TGM deposition flux

The average (range) fluxes of atmospheric Hg deposition at S1, S2, S3, S4, S5 and S6 were 236 (−171–978) mg m^{-2} y^{-1}, 62 (−44–193) mg m^{-2} y^{-1}, 39 (2.9–118) mg m^{-2} y^{-1}, 63 (−151–219) mg m^{-2} y^{-1}, 7.7 (−19–34) mg m^{-2} y^{-1} and 0.59 (−16–19) mg m^{-2} y^{-1}, respectively. The deposition fluxes of atmospheric Hg in the Xunyang Hg mining district decreased with increasing distance from the smelter. The highest deposition flux of atmospheric Hg was observed at S1, which was adjacent to the smelter. As shown in Fig. 2, the deposition fluxes of atmospheric Hg at S6 exhibited small variations with time compared with the polluted sites (S1~S5). The deposition fluxes of atmospheric Hg in the Xunyang Hg mining district (S1~S5) were 1–3 orders of magnitude higher than that at control site S6, indicating that Hg emissions from the local Hg retorting facility was the predominant contribution to the Hg in surface soils in the Xunyang Hg mining district.

During our sampling period, the atmospheric Hg deposition flux constantly changed at each site, but no clear seasonal variations were observed (Fig. 2). Previous studies have reported that atmospheric Hg deposition flux is a dynamic cycling process and that the Hg deposited in soils can later be re-emitted as Hg^0, leading to a dynamic exchange of Hg between soil and air (Lindberg et al., 1998; Magarelli and Fostier, 2005; Montoya et al., 2019). Several modelling studies over various spatial scales have reported that approximately 2000 t y^{-1} Hg was released from soil and terrestrial vegetation, of which 75% was from re-emission (Selin et al., 2007). In the present study, the mean value of atmospheric Hg deposition fluxes was positive, indicating that the Hg in the surface soil continuously accumulated in the Xunyang Hg mining district. Hg deposition on terrestrial surfaces from the atmosphere by wet and

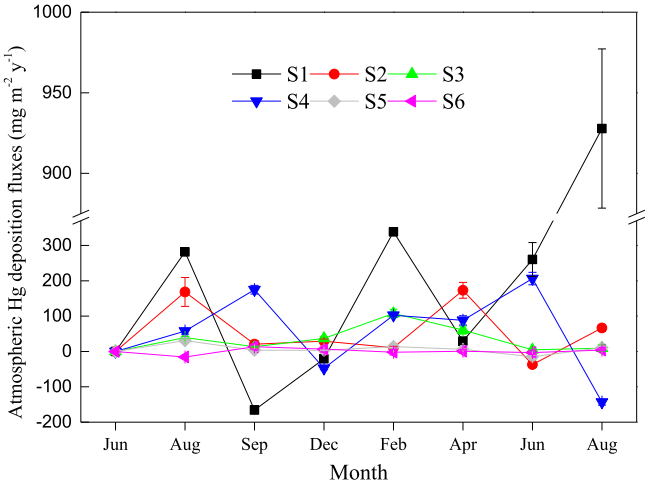

Fig. 2. Atmospheric Hg deposition fluxes during research period.

Table 1
Total gaseous mercury (TGM) concentrations in the ambient air in the Xunyang Hg mining district (ng m^{-3}).

Month	S1		S2		S3		S4		S5		S6	
	Mean	Range	Mean	Range	Mean	Range	Mean	Range	Mean	Range	Mean	Range
Jun	68 ± 8.5	57–92	304 ± 112	191–537	77 ± 8.7	62–108	101 ± 15	68–132	53 ± 4.2	47–61	9.3 ± 1.8	4.0–12
Aug	96 ± 6.6	85–108	407 ± 41	372–525	64 ± 3.6	59–73	27 ± 1.2	25–30	5.1 ± 1.1	2.0–7.0	2.6 ± 0.93	2.0–6.0
Sep	257 ± 60	140–370	91 ± 8.6	81–117	23 ± 3.7	14–28	100 ± 28	66–173	8.4 ± 1.4	5.4–12	3.2 ± 1.0	0.64–5.1
Dec	42 ± 3.1	29–52	36 ± 14	15–81	26 ± 4.8	14–37	18 ± 3.4	8.4–26	18 ± 4.5	7.8–29	8.9 ± 2.3	2.8–15
Feb	16 ± 3.3	8.8–22	99 ± 18	73–128	27 ± 5.7	15–40	15 ± 2.6	11–24	3.8 ± 0.99	1.1–6.3	3.2 ± 0.74	2.0–5.2
Apr	108 ± 5.4	96–118	187 ± 17	151–216	31 ± 5.6	23–44	28 ± 4.5	22–52	24 ± 0.79	22–26	4.4 ± 0.84	1.8–5.8
Jun	21 ± 6.3	11–37	188 ± 37	130–272	4.2 ± 0.95	1.7–6.4	21 ± 3.0	15–28	6.5 ± 1.4	3.0–9.5	6.7 ± 1.9	2.3–10
Aug	6.4 ± 0.63	4.2–8.1	238 ± 80	94–418	6.8 ± 1.2	3.3–9.3	19 ± 3.0	13–26	6.9 ± 1.1	5.0–10	7.6 ± 0.74	5.7–9.5
Mean	77 ± 82	2.6–370	193 ± 122	62–537	32 ± 27	1.7–108	41 ± 37	8.4–173	16 ± 17	2.0–61	5.7 ± 2.7	2.1–15

dry processes is a dominant process in this region.

The deposition fluxes of atmospheric Hg in the Xunyang Hg mining district were compared with data from the literature for different regions, such as urban, rural and industrial areas. The atmospheric Hg deposition fluxes in the Xunyang Hg mining district (S1~S5) were 1–2 orders of magnitude greater than those in Guiyang City (1.2 mg m^{-2} y^{-1}, Tan et al., 2000), Zunyi City (2.3 mg m^{-2} y^{-1}, Tan et al., 2000), Changchun City (0.32 mg m^{-2} y^{-1}, Fang et al., 2004) and the Pearl River Delta Region, China (0.16 mg m^{-2} y^{-1}, Liu et al., 2018), which are typical industrial cities in China. The deposition flux of atmospheric Hg at the control site S6 was similar level to the reported global atmospheric Hg deposition flux of 0.5 mg m^{-2} y^{-1} (Dominguez et al., 2001), suggesting that the control site S6 was less affected by the smelter in the study region. However, the deposition flux of atmospheric Hg at control site S6 was still relatively high compared to remote regions around the world, such as Changbai Mountain (24.9 μg m^{-2} y^{-1}, Wan et al., 2009b), Leigong Mountain (56 μg m^{-2} y^{-1}, Tan et al., 2000) and Hokkaido (10 μg m^{-2} y^{-1}, Sakata and Marumoto, 2005). Obviously, the atmospheric Hg deposition fluxes in the Xunyang Hg mining area were significantly higher than those reported in the regions mentioned above, indicating that the ambient air and surrounding environment in the Xunyang Hg mining district suffered from serious Hg contamination.

4.1.3. Regional Hg loading

Based on the atmospheric Hg deposition fluxes, the annual Hg loading in the Xunyang Hg mining district was estimated to be approximately 10 t y^{-1}, the annual Hg loading in the circular areas of S1, S2, S3, S4, S5 and S6 were 0.19 t y^{-1}, 0.39 t y^{-1}, 1.7 t y^{-1}, 3.9 t y^{-1}, 3.1 t y^{-1} and 0.99 t y^{-1}, respectively (Fig. 3). Statistical analysis showed that distances of 6.0–12 km from the retorting facility were the most important areas for deposition of atmospheric Hg, with levels as high as 7.0 t y^{-1}, and accounting for approximately 85% of the total annual Hg loading in the study area. The Hg loading was mainly related to the distance from the Hg retorting centre as well as the meteorological conditions and topographic features (Csavina et al., 2011; Li et al., 2017). Generally, the Asian monsoon provides warm humid southeast winds during wet seasons (summer and autumn), while cold dry northwest winds during dry seasons (spring and winter) dominate the large-scale wind system in the Xunyang Hg mining district (Fig. 1). The meteorological conditions during the wet seasons (summer and autumn) are generally humid with abundant precipitation and dense vegetation, which may promote the deposition of atmospheric Hg in the Xunyang Hg mining district (Pan and Wang, 2015). However, the relatively low precipitation combined with strong winds and a lack of vegetation during the dry seasons (spring and winter) may favour the resuspension of soil particles in the atmosphere, thus increasing the dry deposition of Hg in the study area (Chen et al., 2014; Louis et al., 2019). In addition, the topographic and physiographic characteristics are regarded as important factors controlling the prevalence of different air circulations (Castillo et al., 2013). The Xunyang Hg mining district is blocked by the Qinling Mountain. Therefore, the northwest wind associated with the channeling of airflows along the mountain valley is predominant during the dry seasons (spring and winter) in the study area, which may stimulate the deposition of atmospheric

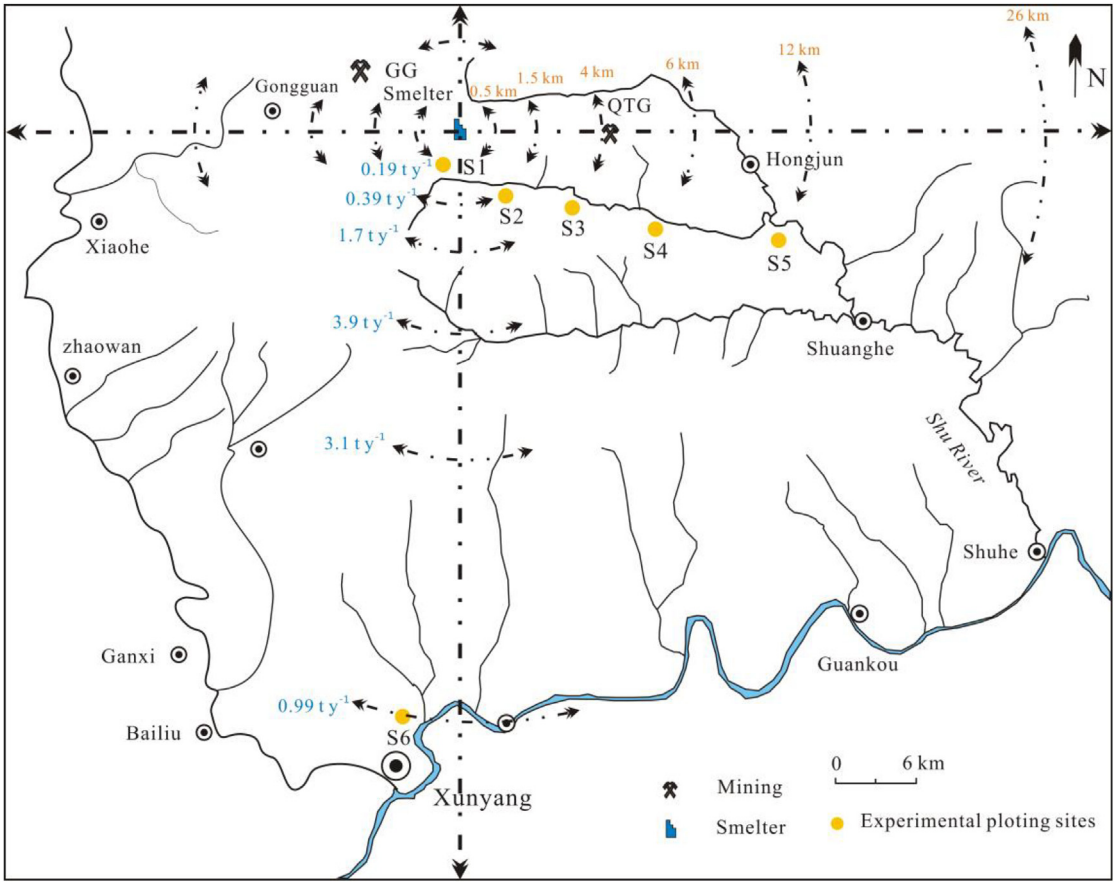

Fig. 3. Estimation of atmospheric Hg deposition loading in Xunyang Hg mining district.

Hg to the local terrestrial ecosystems.

Preliminary measurements and modelling analyses showed that the annual dry and wet Hg loading for East Asia in 2001 was in the range of 590–735 t and 482–696 t, respectively (Pan et al., 2010). Wang et al. (2018) reported that the total Hg deposition in Mainland China was estimated to be 422 t y^{-1}, with wet deposition accounting for nearly half (49%) of the total deposition, and approximately two thirds of the deposition was contributed by domestic emissions. Dai et al. (2013) reported that the masses of Hg in soil induced by anthropogenic sources were 1227 t in arable soil and 75 t in natural soil in the Wanshan catchment. Global models have suggested that the surface soil Hg reservoir may have increased by 15% since industrialization and the land emissions included prompt recycling of recently deposited Hg (600 t y^{-1}) and soil volatilization (550 t y^{-1}) (Selin et al., 2008). Although the annual Hg loading in the Xunyang Hg mining area accounted for a small part of the total in East Asia, the atmospheric Hg deposition fluxes of 7.7–236 mg m^{-2} y^{-1} were significantly higher than the values of 10–160 μg m^{-2} y^{-1} for East Asia (Pan et al., 2010), suggesting that the dominant Hg loading impacts the local surroundings rather than the regional and global areas. Since the methylation of newly deposited Hg in paddy soils constitutes a key step in the cycling of Hg and is a significant source of MeHg in downstream water bodies, the high local Hg loading raises an important concern regarding the potential effects of this biogeochemical process.

4.2. Soil

4.2.1. THg

THg concentrations in soils collected from the experimental pots at five sites (except for S6) during the study period exhibited an increasing trend (Fig. 4a). Within 14 months of exposure to atmospheric deposition, the average THg concentrations in the soils for S1, S2, S3, S4 and S5 were 1.6 ± 0.97 mg kg^{-1}, 0.93 ± 0.22 mg kg^{-1}, 0.73 ± 0.25 mg kg^{-1}, 0.90 ± 0.33 mg kg^{-1} and 0.43 ± 0.017 mg kg^{-1}, respectively, which increased by 3.8, 1.8, 1.2, 1.7 and 0.3 times, respectively, compared with the THg concentration of 0.33 ± 0.0029 mg kg^{-1} in the original soil. All soils from these five experimental pots exhibited THg concentrations greater than the value of 0.34 ± 0.022 mg kg^{-1} observed at S6, which showed little change with time compared to its original soil. This phenomenon implies that atmospheric Hg deposition on surface soils adjacent to the Hg retorting facility intensified, and the highest values of THg in soils observed at S1 adjacent to the Hg retorting facility, suggested that this facility was the dominant source of Hg in the soils. Statistical analysis also revealed a significantly positive correlation between TGM in the ambient air and soil THg ($r = 0.50$, $p < 0.05$, Fig. 5a). The high TGM concentrations in the ambient air cause high Hg in soils, indicating that the soil-rice ecosystem is a net Hg deposition pool in the region.

During rice growing periods, the experimental paddy soils were flooded and received Hg from atmospheric deposition. Although rice may absorb Hg from soils and re-emission caused by the photoreduction of Hg^{2+} in soils might occur (Gillis, 2000; Song and Heyst, 2005; Wang et al., 2007), the elevated high TGM concentrations in the ambient air caused high deposition rates of TGM, resulting in greater Hg deposition than that due to re-emission. Hence, the dynamic process of deposition and re-emission could eventually cause increased Hg in paddy soils. After the rice harvest (September), the increased incident light would promote the release of Hg^0 into the air (Gustin and Stamenkovic, 2005). In the winter season (from December to March), the amount of Hg released with the continuous reduction in temperature decreased (Gustin and Stamenkovic, 2005), so that the Hg content in soil increased with the increasing deposited time.

4.2.2. MeHg

The distribution patterns of MeHg in the experimental soils are shown in Fig. 4b. After 14 months, the mean MeHg concentrations

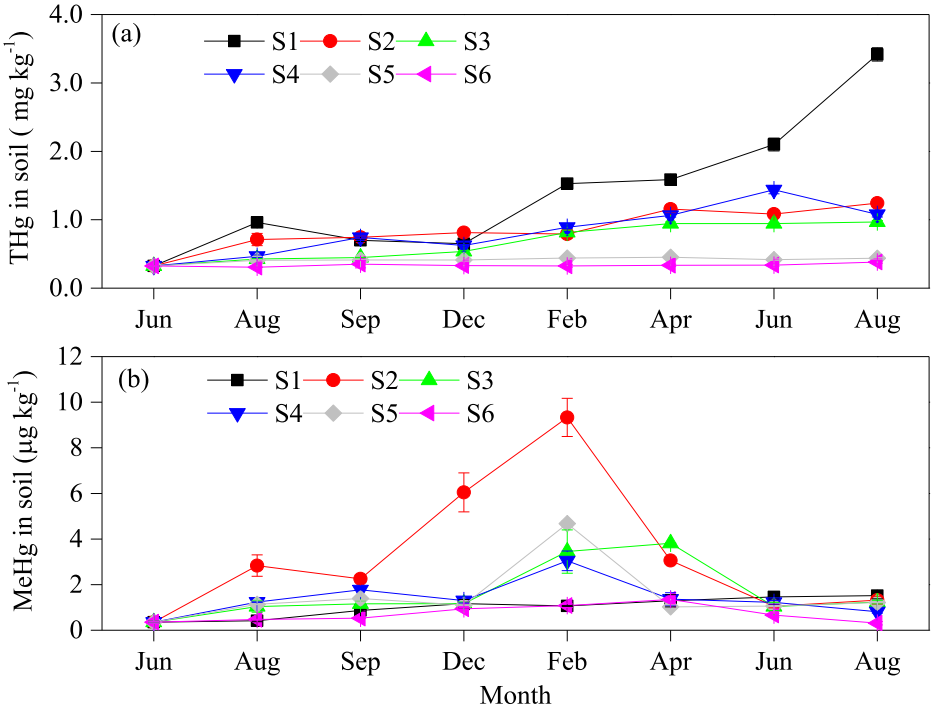

Fig. 4. Monthly variations of THg and MeHg concentrations in experimental soils.

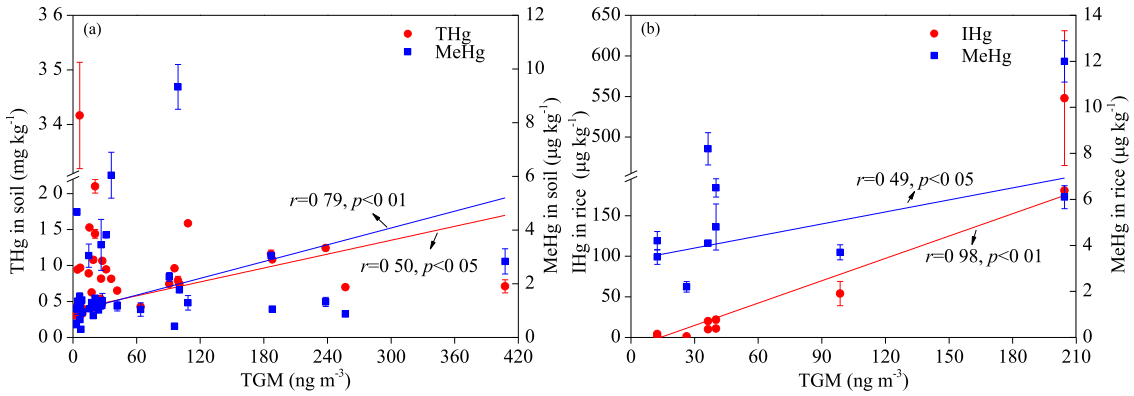

Fig. 5. Correlations between TGM and THg and MeHg in soils as well as IHg and MeHg in rice.

in the tested soils for S1, S2, S3, S4 and S5 were 1.1 ± 0.38 μg kg^{-1}, 3.7 ± 2.9 μg kg^{-1}, 1.8 ± 1.2 μg kg^{-1}, 1.5 ± 0.72 μg kg^{-1} and 1.7 ± 1.3 μg kg^{-1}, respectively. Compared with those of the control site S6 (0.76 ± 0.37 μg kg^{-1}) and original soil (0.38 ± 0.09 μg kg^{-1}), the MeHg concentrations in soils from sites S1, S2, S3, S4, and S5 that were directly impacted by the Hg retorting facility were high. Interestingly, we observed that the distribution pattern of MeHg was unlike the increasing pattern of THg in soils, which showed apparent fluctuations during the experimental period, first increasing and then sharply decreasing (Fig. 4b). From the beginning of the first experimental rice cultivation season, MeHg concentrations in paddy soils continuously increased from June to August 2012 and then increased sharply and reached a peak value in February 2013. Then, the MeHg concentrations in the soils gradually decreased from February to June 2013 (Fig. 4b).

During the rice growing season and as biomass increased, the newly formed MeHg in soils was continuously absorbed by rice and probably caused MeHg equilibrium in soils at a relatively stable MeHg level. Shortly after rice harvesting, the process of MeHg uptake by rice ceased; however, the methylation process was always active and thus increased the MeHg concentrations in the soils. Moreover, the highest concentrations of MeHg production rates observed in February in the present study might also likely reflect postharvest litter decay. The average concentrations of organic matter in the soils increased from $5.8 \pm 0.26\%$ to $6.2 \pm 0.38\%$, which was attributed to rice straw decay. Rice straw decay may also release accumulated MeHg back into the soils; the decay process can promote MeHg production by supplying microbial labile carbon and/or divalent Hg (Marvin-DiPasquale et al., 2014; Windham-Myers et al., 2014; Tomiyasu et al., 2017). This effect can be interpreted as the MeHg peak occurring in soils during the postharvest period.

High proportions of MeHg to THg were observed in the experimental soils, ranging from 0.04% to 1.2%, with an average of $0.25 \pm 0.24\%$. These values were higher than those observed in local paddy soils, which ranged from 0.003% to 0.15%, with an average of $0.04 \pm 0.05\%$. Statistical analysis showed a significant positive correlation between TGM and MeHg in soil ($r = 0.79$, $p < 0.01$, Fig. 5a), indicating that methylated Hg in soil was significantly related to the newly deposited Hg. Our results agree with results that have reported that newly deposited Hg was more reactive than native Hg and was easily transformed to MeHg (Hintelmann et al., 2002; Branfireun et al., 2005; Harris et al., 2007; Meng et al., 2011; Zhao et al., 2016).

4.3. Rice

4.3.1. THg

The concentrations of THg in rice from the experimental pots at the six sites in two harvesting seasons are shown in Table 2. In 2012, the concentrations of THg in rice varied from 1.4 to 186 μg kg^{-1} with a mean of 41 μg kg^{-1} (n = 18). In 2013, the concentrations of THg in rice exhibited a sharp increase, varying from 5.8 to 643 μg kg^{-1} with a mean of 172 μg kg^{-1} (n = 12). Compared to 2012, the average concentrations of THg in rice in 2013 was 4.2 times higher. The maximum THg concentrations in rice were found at S2 during both 2012 and 2013, reaching up to 166 ± 21 μg kg^{-1} and 624 ± 26 μg kg^{-1}, respectively, which significantly exceeded the maximum permissible limit of 20 μg kg^{-1} recommended by the Chinese National Standard Agency (CNSA, 2017). In addition to S2, rice from S3 and S4 also exhibited high THg concentrations as well as a large increase in the second year. Among the six sites, control site S6 showed low concentrations of THg in rice, but these concentrations still increased slightly in the second year.

As S2 was very close to the Hg retorting facility, such elevated THg levels in rice indicated that deposited atmospheric Hg can cause significant Hg accumulation in rice (Bullock et al., 1998; Xu et al., 2017). Previous studies have shown that THg and MeHg concentrations in local paddy soils and rice varied from 5.4 to 120 mg kg^{-1} and from 57 to 200 μg kg^{-1}, respectively (Qiu et al., 2012). Compared with the soil concentrations as high as 120 mg kg^{-1}, the experimental soil in the present study had much lower THg concentrations, even at S2 (1.6 ± 0.97 mg kg^{-1}), which was heavily impacted by atmospheric Hg deposition. However, the rice from the experimental pots at S2 exhibited much higher THg concentrations, which were approximately 3 times higher than the reported peak value of 200 μg kg^{-1}. This phenomenon indicated that the newly deposited Hg is more bioavailable and is more readily taken up by rice. Therefore, effective solutions to reduce the effects from atmospheric deposition should be undertaken, such as substitution, safe utilization and water management. It is important to further reduce the newly deposited Hg into the food chain pose a threat to ecosystems and human health.

4.3.2. MeHg

The average MeHg concentration was 4.2 ± 1.3 (1.9–6.2) μg kg^{-1} (n = 18) in the first year and 7.5 ± 3.6 (1.6–13) μg kg^{-1} (n = 12) in the second year (Table 2). The average MeHg concentration in the rice samples in the second year was 1.8 times higher than in the first year, implying an increase in MeHg accumulation in the simulated rice ecosystem in the active Hg mining region. Elevated

Table 2
Concentrations of THg and MeHg in rice collected from six experimental sites in 2012 and 2013.

Experimental sites	THg ($\mu g\ kg^{-1}$)				MeHg ($\mu g\ kg^{-1}$)			
	2012		2013		2012		2013	
	Mean	Range	Mean	Range	Mean	Range	Mean	Range
S1	52 ± 16	37–71	–	–	3.7 ± 0.33	3.4–3.9	–	–
S2	166 ± 21	145–186	624 ± 26	606–643	2.8 ± 0.07	2.8–2.8	12 ± 0.90	10–13
S3	5.5 ± 0.78	4.8–6.5	28 ± 0.54	28–29	4.1 ± 0.09	4.0–4.1	8.1 ± 0.14	8.0–8.2
S4	15 ± 1.2	13–17	27 ± 5.7	22–33	5.1 ± 1.0	4.1–6.2	6.4 ± 0.18	6.2–6.5
S5	2.9 ± 0.97	1.4–4.1	–	–	2.2 ± 0.24	1.9–2.4	–	–
S6	4.5 ± 0.87	3.5–5.6	7.9 ± 0.85	7.3–8.5	4.2 ± 0.40	3.7–4.5	3.5 ± 0.33	3.2–3.7

Note: the rice grain samples at S1 and S5 sites were not collected in 2013.

MeHg concentrations in rice were found at S2, with peak values reaching 13 $\mu g\ kg^{-1}$, adjacent to the Hg retorting facility. In contrast, MeHg concentrations in rice collected from S6 showed no variation during the two harvest seasons, indicating that these sites were less impacted by the Hg retorting activity compared to the other experimental sites in the present study.

Positive correlations between TGM in the ambient air and MeHg and IHg in rice were observed in the present study (Fig. 5b). The correlation between TGM and IHg ($r = 0.98$, $p < 0.01$) was more significant than that between TGM and MeHg ($r = 0.49$, $p < 0.05$). Generally, rice mainly absorbed MeHg from paddy soils (Meng et al., 2010); however, for IHg, rice can take Hg^{2+} from the soil and absorb Hg^0 from the atmosphere (Fay and Gustin, 2006). Hence, the elevated high atmospheric Hg levels for the experimental sites can become an important Hg source for the aboveground parts of rice plants. The significant positive correlation between rice IHg and TGM might also be interpreted as a pool of increased newly deposited Hg, which is considered for more bioavailable Hg forms (Zhou et al., 2014; Tang et al., 2017). These phenomena suggest that TGM plays a key role in the Hg biogeochemical cycles in the simulated rice ecosystem in the present study. Previous research has reported that, for MeHg, root absorption is the most important pathway for entry into plants, even at low concentrations in soils (Qiu et al., 2008). Moreover, MeHg in rice grains can be transferred into the human body via the food chain and eventually poses a threat to human health. Consequently, it is necessary to take effective measures to reduce Hg emissions into the atmosphere in the Xunyang Hg mining district to protect human health and achieve sustainable development.

5. Conclusions

This study revealed significant TGM contamination and biogeochemical effects of newly deposited TGM in a simulated rice ecosystem in the Xunyang Hg mining district, Shaanxi Province, China. The highest concentrations of TGM were found in the vicinity of the Hg retorting facility, indicating that the TGM was related to the Hg^0 emissions during the process of cinnabar retorting. The annual deposition loading in the Xunyang Hg mining district was approximately 10 t y^{-1}, and the distances of 6.0–12 km from the retorting facility contributed the most important depositional area for atmospheric Hg, accounting for approximately 85% of the total atmospheric Hg loading in this study area. Simulated rice ecosystem experiments demonstrated that significant temporal variations in THg and MeHg in soil were observed during the rice growing season. The soil THg concentrations increased with increased durations of atmospheric deposition, while the MeHg concentrations fluctuated, with a peak value recorded in winter. Elevated concentrations of 643 $\mu g\ kg^{-1}$ THg and 13 $\mu g\ kg^{-1}$ MeHg were observed in rice, which significantly exceeded the maximum THg concentration of 20 $\mu g\ kg^{-1}$ recommended by the Chinese National Standard Agency for food. The results indicated that the newly deposited Hg in experimental soils was more bioavailable, readily methylated, and easily taken up by rice compared to native Hg in local paddy soils. The current study suggests that the ongoing Hg mining activities cause serious Hg contamination to local surface terrestrial ecosystems and pose a potential threat to the population.

Acknowledgements

This study was supported by the National Natural Science Foundation of China (No.41573135, 41703130, 41673025 and U1612442) and by Natural Science Research Project of Guizhou Provincial Education Office (KY2016011). Finally, we are grateful for the support of all persons involved in the project.

Appendix A. Supplementary data

Supplementary data to this article can be found online at https://doi.org/10.1016/j.chemosphere.2019.124630.

References

Ao, M., Meng, B., Sapkota, A., Wu, Y.G., Qian, X.L., Qiu, G.L., Zhong, S.Q., Shang, L.H., 2017. The influence of atmospheric Hg on Hg contaminations in rice and paddy soil in the Xunyang Hg mining district, China. Acta. Geochim. 36 (2), 181–189. https://doi.org/10.1007/s11631-017-0142-x.

Beckers, F., Rinklebe, J., 2017. Cycling of mercury in the environment: sources, fate, and human health implications: a review. Crit. Rev. Environ. Sci. Technol. 47 (9), 693–794. https://doi.org/10.1080/10643389.2017.1326277.

Branfireun, B.A., Krabbenhoft, D.P., Hintelmann, H., Hunt, R.J., Hurley, J.P., Rudd, J.W.M., 2005. Speciation and transport of newly deposited mercury in a boreal forest wetland: a stable mercury isotope approach. Water Resour. Res. 41 (6), W06016. https://doi.org/10.1029/2004wr003219.

Bullock, O.R., Brehme, K.A., Mapp, G.R., 1998. Lagrangian modeling of mercury air emission, transport and deposition: an analysis of model sensitivity to emissions uncertainty. Sci. Total Environ. 213 (1–3), 1–12. https://doi.org/10.1016/s0048-9697(98)00066-7.

Castillo, S., Rosa, J.D.D.L., Campa, A.M.S.D.L., González-Castanedo, Y., Fernández-Camacho, R., 2013. Heavy metal deposition fluxes affecting an Atlantic coastal area in the southwest of Spain. Atmos. Environ. 77, 509–517. https://doi.org/10.1016/j.atmosenv.2013.05.046.

Chen, Y., Schleicher, N., Chen, Y.Z., Chai, F.H., Norra, S., 2014. The influence of governmental mitigation measures on contamination characteristics of PM2.5 in Beijing. Sci. Total Environ. 490, 647–658. https://doi.org/10.1016/j.scitotenv.2014.05.049.

Clarkson, T.W., Magos, L., Myers, G.J., 2003. The toxicology of mercury-current exposures and clinical manifestations. N. Engl. J. Med. 349 (18), 1731–1737. https://doi.org/10.1056/nejmra022471.

CNSA, 2017. Chinese standards for food quality. Chinese National Standard Agency, GB2762–2017 (in Chinese). http://bz.cfsa.net.cn/staticPages/D5921FFE-BD08-4D34-AE26-CF9CA4FEB001.html.

Csavina, J., Landázuri, A., Wonaschütz, A., Rine, K., Rheinheimer, P., Barbaris, B., Conant, W., Sáez, A.E., Betterton, E.A., 2011. Metal and metalloid contaminants in atmospheric aerosols from mining operations. Water, Air, Soil Pollut. 221 (1–4), 145–157. https://doi.org/10.1007/s11270-011-0777-x.

Dai, Z.H., Feng, X.B., Zhang, C., Wang, J.F., Jiang, T.M., Xiao, H.J., Li, Y., Wang, X.,

Qiu, G.L., 2013. Assessing anthropogenic sources of mercury in soil in Wanshan Hg mining area, Guizhou, China. Environ. Sci. Pollut. Res. 20 (11), 7560–7569. https://doi.org/10.1007/s11356-013-1616-y.
Dominguez, A., Gutierrez, M., Vazquez, F.A., 2001. Quantitative evaluation of atmospheric deposition flux of mercury in sediments within the city of Juarez, Mexico. Water. Air. Soil. Pollut. 132 (3–4), 263–274. https://doi.org/10.1023/a:1013298630997.
Driscoll, C.T., Mason, R.P., Chan, H.M., Jacob, D.J., Pirrone, N., 2013. Mercury as a global pollutant: sources, pathways, and effects. Environ. Sci. Technol. 47 (10), 4967–4983. https://doi.org/10.1021/es305071v.
Fang, F.M., Wang, Q.C., Li, J.F., 2004. Urban environmental mercury in Changchun, a metropolitan city in Northeastern China: source, cycle, and fate. Sci. Total Environ. 330 (1–3), 159–170. https://doi.org/10.1016/j.scitotenv.2004.04.006.
Fay, L., Gustin, M., 2006. Assessing the influence of different atmospheric and soil mercury concentrations on foliar mercury concentrations in a controlled environment. Water, Air, Soil Pollut. 181 (1–4), 373–384. https://doi.org/10.1007/s11270-006-9308-6.
Feng, X.B., Li, P., Qiu, G.L., Wang, S.F., Li, G.H., Shang, L.H., Meng, B., Jiang, H.M., Bai, W.Y., Li, Z.G., Fu, X.W., 2008. Human exposure to methylmercury through rice intake in mercury mining areas, Guizhou Province, China. Environ. Sci. Technol. 42 (1), 326–332. https://doi.org/10.1021/es071948x.
Ferrat, M., Weiss, D.J., Dong, S., Large, D.J., Spiro, B., Sun, Y., Gallagher, K., 2012. Lead atmospheric deposition rates and isotopic trends in Asian dust during the last 9.5 kyr recorded in an ombrotrophic peat bog on the eastern Qinghai–Tibetan Plateau. Geochem. Cosmochim. Acta 82, 4–22. https://doi.org/10.1016/j.gca.2010.10.031.
Fu, X.W., Feng, X.B., Sommar, J., Wang, S.F., 2012. A review of studies on atmospheric mercury in China. Sci. Total Environ. 421–422, 73–81. https://doi.org/10.1016/j.scitotenv.2011.09.089.
Galbreath, K.C., Zygarlicke, C.J., 1996. Mercury speciation in coal combustion and gasification flue gases. Environ. Sci. Technol. 30 (8), 2421–2426. https://doi.org/10.1021/es950935t.
Gibb, H., Haver, C., Kozlov, K., Centeno, J.A., Jurgenson, V., Kolker, A., Conko, K.M., Landa, E.R., Xu, H., 2011. Biomarkers of mercury exposure in two eastern Ukraine Cities. J. Occup. Environ. Hyg. 8 (4), 187–193. https://doi.org/10.1080/15459624.2011.556984.
Gillis, A., 2000. Some local environmental effects on mercury emission and absorption at a soil surface. Sci. Total Environ. 260 (1–3), 191–200. https://doi.org/10.1016/s0048-9697(00)00563-5.
Gustin, M.S., Stamenkovic, J., 2005. Effect of watering and soil moisture on mercury emissions from soils. Biogeochemistry (Dordr.) 76 (2), 215–232. https://doi.org/10.1007/s10533-005-4566-8.
Harris, R.C., Rudd, J.W.M., Amyot, M., Babiarz, C.L., Beaty, K.G., Blanchfield, P.J., Bodaly, R.A., Branfireun, B.A., Gilmour, C.C., Graydon, J.A., Heyes, A., Hintelmann, H., Hurley, J.P., Kelly, C.A., Krabbenhoft, D.P., Lindberg, S.E., Mason, R.P., Paterson, M.J., Podemski, C.L., Robinson, A., Sandilands, K.A., Southworth, G.R., Louis, V.L.S., Tate, M.T., 2007. Whole-ecosystem study shows rapid fish-mercury response to changes in mercury deposition. Proc. Natl. Acad. Sci. 104 (42), 16586–16591. https://doi.org/10.1073/pnas.0704186104.
Hintelmann, H., Harris, R., Heyes, A., Hurley, J.P., Kelly, C.A., Krabbenhoft, D.P., Lindberg, S., Rudd, J.W.M., Scott, K.J., StLouis, V.L., 2002. Reactivity and mobility of new and old mercury deposition in a boreal forest ecosystem during the first year of the METAALICUS study. Environ. Sci. Technol. 36 (23), 5034–5040. https://doi.org/10.1021/es025572t.
Jaffe, D., Strode, S., 2008. Sources, fate and transport of atmospheric mercury from Asia. Environ. Chem. 5 (2), 121–126. https://doi.org/10.1071/en08010.
Kocman, D., Vreča, P., Fajon, V., Horvat, M., 2011. Atmospheric distribution and deposition of mercury in the Idrija Hg mine region, Slovenia. Environ. Res. 111 (1), 1–9. https://doi.org/10.1016/j.envres.2010.10.012.
Li, P., Feng, X.B., Yuan, X., Chan, H.M., Qiu, G.L., Sun, G.X., Zhu, Y.G., 2012a. Rice consumption contributes to low level methylmercury exposure in southern China. Environ. Int. 49, 18–23. https://doi.org/10.1016/j.envint.2012.08.006.
Li, P., Feng, X.B., Qiu, G.L., Shang, L.H., Wang, S.F., 2012b. Mercury pollution in Wuchuan mercury mining area, Guizhou, Southwestern China: the impacts from large scale and artisanal mercury mining. Environ. Int. 42, 59–66. https://doi.org/10.1016/j.envint.2011.04.008.
Li, S., Li, Y., Liang, H.D., Wang, Z.Y., Xue, Y.L., 2014. Atmospheric mercury emissions from domestic coal and impacts on local environment of suburban Beijing (in Chinese). Res. Environ. Sci. 27 (12), 1420–1425. https://doi.org/10.13198/j.Issn.1001-6929.2014.12.05.
Li, X., Yang, H., Zhang, C., Zeng, G.M., Liu, Y.G., Xu, W.H., Wu, Y.E., Lan, S.M., 2017. Spatial distribution and transport characteristics of heavy metals around an antimony mine area in central China. Chemosphere 170, 17–24. https://doi.org/10.1016/j.chemosphere.2016.12.011.
Liang, L., Horvat, M., Cernichiari, E., Gelein, B., Balogh, S., 1996. Simple solvent extraction technique for elimination of matrix interferences in the determination of methylmercury in environmental and biological samples by ethylation-gas chromatography-cold vapor atomic fluorescence spectrometry. Talanta 43 (11), 1883–1888. https://doi.org/10.1016/0039-9140(96)01964-9.
Liang, L., Horvat, M., Feng, X.B., Shang, L.H., Li, H., Pang, P., 2004. Re-evaluation of distillation and comparison with HNO_3 leaching/solvent extraction for isolation of methylmercury compounds from sediment/soil samples. Appl. Organomet. Chem. 18 (6), 264–270. https://doi.org/10.1002/aoc.617.
Lin, L.Y., Chang, L.F., Jiang, S.J., 2008. Speciation analysis of mercury in cereals by liquid chromatography chemical vapor generation inductively coupled plasma-mass spectrometry. J. Agric. Food Chem. 56 (16), 6868–6872. https://doi.org/10.1021/jf801241w.
Lindberg, S.E., Hanson, P.J., Meyers, T.P., Kim, K.H., 1998. Air/surface exchange of mercury vapor over forests-the need for a reassessment of continental biogenic emissions. Atmos. Environ. 32 (5), 895–908. https://doi.org/10.1016/s1352-2310(97)00173-8.
Lindberg, S., Bullock, R., Ebinghaus, R., Engstrom, D., Feng, X.B., Fitzgerald, W., Pirrone, N., Prestbo, E., Seigneur, C., 2007. A synthesis of progress and uncertainties in attributing the sources of mercury in deposition. AMBIO A J. Hum. Environ. 36 (1), 19–33. https://doi.org/10.1579/0044-7447(2007)36[19:asopau]2.0.co;2.
Lindqvist, O., Johansson, K., Bringmark, L., Timm, B., Aastrup, M., Andersson, A., Bringmark, L., Hovsenius, G., Hakanson, L., Iverfeldt, A., Meili, M., Timm, B., 1991. Mercury in the Swedish environment ? Recent research on causes, consequences and corrective methods. Water, Air, Soil Pollut. 55 (1–2) xi–261. https://doi.org/10.1007/bf00542429.
Liu, N., Qiu, G.L., Landis, M.S., Feng, X.B., Fu, X.W., Shang, L.H., 2011. Atmospheric mercury species measured in Guiyang, Guizhou province, southwest China. Atmos. Res. 100 (1), 93–102. https://doi.org/10.1016/j.atmosres.2011.01.002.
Liu, J.J., Wang, L., Zhu, Y., Lin, C.J., Jang, C., Wang, S.X., Xing, J., Yu, B., Xu, H., Pan, Y.Z., 2018. Source attribution for mercury deposition with an updated atmospheric mercury emission inventory in the Pearl River Delta Region, China. Front. Environ. Sci. Eng. 13 (1). https://doi.org/10.1007/s11783-019-1087-6.
Liu, H.L., Zhou, J., Li, M., Hu, Y., Liu, X., Zhou, J., 2019. Study of the bioavailability of heavy metals from atmospheric deposition on the soil-pakchoi (Brassica chinensis L.) system. J. Hazard Mater. 362, 9–16. https://doi.org/10.1016/j.jhazmat.2018.09.032.
Louis, V.L.S., Graydon, J.A., Lehnherr, I., Amos, H.M., Sunderland, E.M., Pierre, K.A.S., Emmerton, C.A., Sandilands, K., Tate, M., Steffen, A., Humphreys, E.R., 2019. Atmospheric concentrations and wet/dry loadings of mercury at the remote experimental lakes area, Northwestern Ontario, Canada. Environ. Sci. Technol. 53 (14), 8017–8026. https://doi.org/10.1021/acs.est.9b01338.
Ma, M., Wang, D., Du, H., Sun, T., Zhao, Z., Wei, S., 2015. Atmospheric mercury deposition and its contribution of the regional atmospheric transport to mercury pollution at a national forest nature reserve, southwest China. Environ. Sci. Pollut. Res. 22 (24), 20007–20018. https://doi.org/10.1007/s11356-015-5152-9.
Magarelli, G., Fostier, A.H., 2005. Influence of deforestation on the mercury air/soil exchange in the Negro River Basin, Amazon. Atmos. Environ. 39 (39), 7518–7528. https://doi.org/10.1016/j.atmosenv.2005.07.067.
Mahaffey, K.R., Clickner, R.P., Bodurow, C.C., 2004. Blood organic mercury and dietary intake: national health and nutrition examination survey, 1999 and 2000. Environ. Health Perspect. 112 (5), 562–569. https://doi.org/10.1289/ehp.6587.
Marvin-DiPasquale, M., Windham-Myers, L., Agee, J.L., Kakouros, E., Kieu, L.H., Fleck, J.A., Alpers, C.N., Stricker, C.A., 2014. Methylmercury production in sediment from agricultural and non-agricultural wetlands in the Yolo Bypass, California, USA. Sci. Total Environ. 484, 288–299. https://doi.org/10.1016/j.scitotenv.2013.09.098.
Meng, B., Feng, X.B., Qiu, G.L., Cai, Y., Wang, D.Y., Li, P., Shang, L.H., Sommar, J., 2010. Distribution patterns of inorganic mercury and methylmercury in tissues of rice (*Oryza sativa* L.) plants and possible bioaccumulation pathways. J. Agric. Food Chem. 58 (8), 4951–4958. https://doi.org/10.1021/jf904557x.
Meng, B., Feng, X.B., Qiu, G.L., Liang, P., Li, P., Chen, C.X., Shang, L.H., 2011. The process of methylmercury accumulation in rice (*Oryza sativa* L.). Environ. Sci. Technol. 45 (7), 2711–2717. https://doi.org/10.1021/es103384v.
Meng, B., Feng, X.B., Qiu, G.L., Wang, D.Y., Liang, P., Li, P., Shang, L.H., 2012. Inorganic mercury accumulation in rice (*Oryza sativa* L.). Environ. Toxicol. Chem. 31 (9), 2093–2098. https://doi.org/10.1002/etc.1913.
Montoya, A.J., Lena, J.C., Windmöller, C.C., 2019. Adsorption of gaseous elemental mercury on soils: influence of chemical and/or mineralogical characteristics. Ecotoxicol. Environ. Saf. 170, 98–106. https://doi.org/10.1016/j.ecoenv.2018.11.054.
Outridge, P.M., Mason, R.P., Wang, F., Guerrero, S., Heimburger, L.E., 2018. Updated global and oceanic mercury budgets for the united nations global mercury assessment 2018. Environ. Sci. Technol. 52 (20), 11466–11477. https://doi.org/10.1021/acs.est.8b01246.
Pan, L., Lin, C.J., Carmichael, G.R., Streets, D.G., Tang, Y., Woo, J.H., Shetty, S.K., Chu, H.W., Ho, T.C., Friedli, H.R., Feng, X.B., 2010. Study of atmospheric mercury budget in East Asia using STEM-Hg modeling system. Sci. Total Environ. 408 (16), 3277–3291. https://doi.org/10.1016/j.scitotenv.2010.04.039.
Pan, Y.P., Wang, Y.S., 2015. Atmospheric wet and dry deposition of trace elements at 10 sites in Northern China. Atmos. Chem. Phys. 15 (2), 951–972. https://doi.org/10.5194/acp-15-951-2015.
Qiu, G.L., Feng, X.B., Wang, S.F., Li, G.H., Shang, L.H., Fu, X.W., 2008. Methylmercury accumulation in rice (*Oryza sativa* L.) grown at abandoned mercury mines in Guizhou, China. J. Agric. Food Chem. 56 (7), 2465–2468. https://doi.org/10.1021/jf073391a.
Qiu, G.L., Feng, X.B., Meng, B., Wang, X., 2011. Methylmercury in rice (*Oryza sativa* L.) grown from the Xunyang Hg mining area, Shaanxi province, northwestern China. Pure Appl. Chem. 84 (2), 281–289. https://doi.org/10.1351/pac-con-11-09-16.
Qiu, G.L., Feng, X.B., Meng, B., Sommar, J., Gu, C.H., 2012. Environmental geochemistry of an active Hg mine in Xunyang, Shaanxi province, appl. Geochem. (Tokyo. 1967) 27 (12), 2280–2288. https://doi.org/10.1016/j.apgeochem.2012.08.003.
Qiu, G.L., Feng, X.B., Meng, B., Zhang, C., Gu, C.H., Du, B.Y., Lin, Y., 2013.

Environmental geochemistry of an abandoned mercury mine in Yanwuping, Guizhou Province, China. Environ. Res. 125, 124–130. https://doi.org/10.1016/j.envres.2013.01.008.
Sakata, M., Marumoto, K., 2005. Wet and dry deposition fluxes of mercury in Japan. Atmos. Environ. 39 (17), 3139–3146. https://doi.org/10.1016/j.atmosenv.2005.01.049.
Schroeder, W.H., Munthe, J., 1998. Atmospheric mercury-An overview. Atmos. Environ. 32 (5), 809–822. https://doi.org/10.1016/s1352-2310(97)00293-8.
Selin, N.E., Jacob, D.J., Park, R.J., Yantosca, R.M., Strode, S., Jaeglé, L., Jaffe, D., 2007. Chemical cycling and deposition of atmospheric mercury: global constraints from observations. J. Geophys. Res. 112 (D2), D02308. https://doi.org/10.1029/2006jd007450.
Selin, N.E., Jacob, D.J., Yantosca, R.M., Strode, S., Jaeglé, L., Sunderland, E.M., 2008. Global 3-D land-ocean-atmosphere model for mercury: present-day versus preindustrial cycles and anthropogenic enrichment factors for deposition. Glob. Biogeochem. Cycles 22 (2) n/a–n/a. https://doi.org/10.1029/2007gb003040.
Song, X.X., Heyst, B.V., 2005. Volatilization of mercury from soils in response to simulated precipitation. Atmos. Environ. 39 (39), 7494–7505. https://doi.org/10.1016/j.atmosenv.2005.07.064.
Sprovieri, F., Pirrone, N., Ebinghaus, R., Kock, H., Dommergue, A., 2010. A review of worldwide atmospheric mercury measurements. Atmos. Chem. Phys. 10 (17), 8245–8265. https://doi.org/10.5194/acp-10-8245-2010.
Tan, H., He, J.L., Liang, L., Lazoff, S., Sommer, J., Xiao, Z.F., Lindqvist, O., 2000. Atmospheric mercury deposition in Guizhou, China. Sci. Total Environ. 259 (1–3), 223–230. https://doi.org/10.1016/s0048-9697(00)00584-2.
Tang, W.L., Dang, F., Evans, D., Zhong, H., Xiao, L., 2017. Understanding reduced inorganic mercury accumulation in rice following selenium application: selenium application routes, speciation and doses. Chemosphere 169, 369–376. https://doi.org/10.1016/j.chemosphere.2016.11.087.
Tomiyasu, T., Kodamatani, H., Imura, R., Matsuyama, A., Miyamoto, J., Akagi, H., Kocman, D., Kotnik, J., Fajon, V., Horvat, M., 2017. The dynamics of mercury near Idrija mercury mine, Slovenia: horizontal and vertical distributions of total, methyl, and ethyl mercury concentrations in soils. Chemosphere 184, 244–252. https://doi.org/10.1016/j.chemosphere.2017.05.123.
Wan, Q., Feng, X.B., Lu, J.Y., Zheng, W., Song, X.J., Han, S.J., Xu, H., 2009a. Atmospheric mercury in Changbai Mountain area, northeastern China I. The seasonal distribution pattern of total gaseous mercury and its potential sources. Environ. Res. 109 (3), 201–206. https://doi.org/10.1016/j.envres.2008.12.001.
Wan, Q., Feng, X.B., Lu, J.Y., Zheng, W., Song, X.J., Li, P., Han, S.J., Xu, H., 2009b. Atmospheric mercury in Changbai Mountain area, northeastern China II. The distribution of reactive gaseous mercury and particulate mercury and mercury deposition fluxes. Environ. Res. 109 (6), 721–727. https://doi.org/10.1016/j.envres.2009.05.006.
Wang, S.F., Feng, X.B., Qiu, G.L., Fu, X.W., Wei, Z., 2007. Characteristics of mercury exchange flux between soil and air in the heavily air-polluted area, eastern Guizhou, China. Atmos. Environ. 41 (27), 5584–5594. https://doi.org/10.1016/j.atmosenv.2007.03.002.
Wang, X., Lin, C.J., Feng, X.B., Yuan, W., Fu, X.W., Zhang, H., Wang, S.X., 2018. Assessment of regional mercury deposition and emission outflow in Mainland China. J. Geophys. Res-Atmos. 123 (17), 9868–9890. https://doi.org/10.1029/2018jd028350.
Weiss-Penzias, P., Jaffe, D.A., McClintick, A., Prestbo, E.M., Landis, M.S., 2003. Gaseous elemental mercury in the marine boundary layer: evidence for rapid removal in anthropogenic pollution. Environ. Sci. Technol. 37 (17), 3755–3763. https://doi.org/10.1021/es0341081.
Windham-Myers, L., Marvin-DiPasquale, M., Kakouros, E., Agee, J.L., Kieu, L.H., Stricker, C.A., Fleck, J.A., Ackerman, J.T., 2014. Mercury cycling in agricultural and managed wetlands of California, USA: seasonal influences of vegetation on mercury methylation, storage, and transport. Sci. Total Environ. 484, 308–318. https://doi.org/10.1016/j.scitotenv.2013.05.027.
Wu, Y., Wang, S.X., Streets, D.G., Hao, J.M., Chan, M., Jiang, J.K., 2006. Trends in anthropogenic mercury emissions in China from 1995 to 2003. Environ. Sci. Technol. 40 (17), 5312–5318. https://doi.org/10.1021/es060406x.
Xu, X.H., Meng, B., Zhang, C., Feng, X.B., Gu, C.H., Guo, J.Y., Bishop, K., Xu, Z.D., Zhang, S.S., Qiu, G.L., 2017. The local impact of a coal-fired power plant on inorganic mercury and methyl-mercury distribution in rice (*Oryza sativa* L.). Environ. Pollut. 223, 11–18. https://doi.org/10.1016/j.envpol.2016.11.042.
Zhao, L., Qiu, G.L., Anderson, C.W.N., Meng, B., Wang, D.Y., Shang, L.H., Yan, H.Y., Feng, X.B., 2016. Mercury methylation in rice paddies and its possible controlling factors in the Hg mining area, Guizhou province, Southwest China. Environ. Pollut. 215, 1–9. https://doi.org/10.1016/j.envpol.2016.05.001.
Zhang, H., Feng, X.B., Larssen, T., Qiu, G.L., Vogt, R.D., 2010a. In inland China, rice, rather than fish, is the major pathway for methylmercury exposure. Environ. Health Perspect. 118 (9), 1183–1188. https://doi.org/10.1289/ehp.1001915.
Zhang, L., Jin, Y.Q., Lu, J.L., Zhang, C.X., 2009. Concentration, distribution and bioaccumulation of mercury in the Xunyang mercury mining area, Shaanxi Province, China. Appl. Geochem. 24 (5), 950–956. https://doi.org/10.1016/j.apgeochem.2009.02.027.
Zhang, L., Wang, S.X., Meng, Y., Hao, J.M., 2012. Influence of mercury and chlorine content of coal on mercury emissions from coal-fired power plants in China. Environ. Sci. Technol. 46 (11), 6385–6392. https://doi.org/10.1021/es300286n.
Zhang, L., Wang, S.X., Wang, L., Wu, Y., Duan, L., Wu, Q.R., Wang, F.Y., Yang, M., Hao, J.M., Liu, X., 2015. Updated emission inventories for speciated atmospheric mercury from anthropogenic sources in China. Environ. Sci. Technol. 49 (5), 3185–3194. https://doi.org/10.1021/es504840m.
Zhang, Y., Chen, Y.J., Qi, J.P., Leng, C.B., Zhao, C.H., 2010b. Geochemistry of gongguanqingtonggou Hg-Sb deposit in Xunyang, Shaanxi province (in Chinese). Acta Mineral. Sin. 30 (1), 98–106. https://doi.org/10.16461/j.cnki.1000-4734.2010.01.017.
Zhou, J., Liu, H.Y., Du, B.Y., Shang, L.H., Yang, J.B., Wang, Y.S., 2014. Influence of soil mercury concentration and fraction on bioaccumulation process of inorganic mercury and methylmercury in rice (*Oryza sativa* L.). Environ. Sci. Pollut. Res. 22 (8), 6144–6154. https://doi.org/10.1007/s11356-014-3823-6.